Materials Research Proceedings **2** (2016) 55-60 doi: http://dx.doi.org/10.21741/9781945291173-10

Comparison of Two X-Ray Residual Stress Measurement Methods: $Sin^2 \psi$ and Cos α, Through the Determination of a Martensitic Steel X-Ray Elastic Constant

D. Delbergue[1,2,a], D. Texier[1,b], M. Lévesque[2,c], P. Bocher[1,d *]

[1]Laboratoire d'Optimisation des Procédés de Fabrication en Aérospatiale (LOPFA), École de technologie supérieure (ÉTS), 1100 Notre-Dame Ouest, Montréal, QC H3C 1K3, Canada

[2]Laboratory for Multi-Scale Mechanics (LM2), École Polytechnique de Montréal, C.P. 6079, Succ. Centre-ville, Montréal, QC H3C 3A7, Canada

[a]dorian.delbergue.1@ens.etsmtl.ca, [b]damien.texier@etsmtl.ca, [c]martin.levesque@polymtl.ca, [d]philippe.bocher@etsmtl.ca

Keywords: X-Ray Diffraction, Residual Stresses, X-Ray Elastic Constant, Single Exposure

Abstract. X-ray diffraction technique for residual stresses measurement is usually associated to the $\sin^2 \psi$ method, a method based on the interception of the diffraction cone and line detectors. To overcome this loss of information, the cos α method is an alternative method which uses a single exposure to collect the entire diffraction cone via a 2D detector. The present paper compares both $\sin^2 \psi$ and cos α methods, through the X-ray elastic constant (XEC) determination of a quenched and tempered martensitic steel. The full-cone measurement method demonstrates a smaller scatter and a better repeatability of the measurements. This latter point is of considerable interest since larger scatter in XEC may result in large variation in residual stress values, especially at high stress levels.

Introduction

Aerospace, automotive, and power industries are constantly looking for means to improve fatigue life. Many surface-treatment processes, such as laser peening or shot peening, are known to improve fatigue life due to introduction of near-surface compressive residual stresses. However, the relationship between processes and fatigue life improvement is not fully understood. These surface-treatment processes introduce a residual stress profile in a shallow region beneath the surface which may delay the crack nucleation and/or propagation. Therefore, residual stresses are more and more accounted for fatigue life prediction models. Consequently, it is of major concern to assess residual stresses with the best possible accuracy. Many characterization techniques, such as hole-drilling, X-ray diffraction (XRD), or ultrasonics, have been developed during the last century to measure them.

X-ray diffraction technique has been widely used in industries and laboratories for residual stresses measurement. The XRD technique is based on the measurement of the crystallographic lattice deformation. According to Bragg conditions, a change in lattice spacing induce a shift of the diffracted X-ray angle [1]. Then, the strain and stress can be calculated from the peak shift. For decades, the traditional $\sin^2 \psi$ method has been employed for stress calculation [2]. The dedicated diffractometer mainly use line detectors, most commonly Position Sensitive Scintillation Detectors (PSSD), in order to capture the scattered X-rays. In the case of stress-free isotropic polycrystalline material, X-rays are diffracted in all directions by the grains, giving form to a cone. The line detectors only capture a limited part of the scattered X-rays corresponding to two diffraction cone radii. In the case of plane-stress state, a minimum of two sample orientations are required for strain measurements [2].

In 1978, the cos α method was developed in Japan for stress calculation [3]. This method, also called the single exposure method, allows stress calculation by capturing the resulting diffraction

Materials Research Proceedings **2** (2016) 55-60 doi: http://dx.doi.org/10.21741/9781945291173-10

cone of a single incident X-ray beam via a 2D detector. The intersection of the diffraction cone with the area detector provides a ring named Debyer-Scherrer ring [1]. The introduction of new 2D photosensitive detectors, such as image plate (IP), and the development of powerful calculation algorithms, bring the cos α method up to date [4]. Since few years, portable apparatus equipped with IP allow quick residual stress measurements using the cos α method.

The two presented XRD methods measure the elastic strain for a chosen diffraction peak corresponding to specific planes of atoms in the crystal structure. This family of planes does not necessarily have the same elastic constants than the bulk material; the latter being the expression of the average elastic behavior of all plane families. Therefore, the X-ray elastic constants (XEC) determination is needed for the chosen peak of the material subjected to X-ray residual stress measurement [5]. The XEC are determined by measuring the lattice strain of given crystallographic planes using a diffractometer while the specimen is subjected to constant axial loading. A wrong XEC value may underestimate the residual stress state, leading to non-conservative fatigue predictions [6, 7].

The present work aims at measuring the XEC with both methods on a quenched and tempered martensitic steel, and test their accuracy and repeatability.

Stress analysis

For both apparatuses, the scattered X-rays are recorded for a specific family of planes {hkl}. When the diffraction peaks have been fitted and the corresponding Bragg's angles determined, the d-spacing (also called the lattice spacing) $d^{\{hkl\}}$ can be calculated using the Bragg's law. The strain is then obtained by Eq. 1:

$$\varepsilon_{\varphi\psi}^{\{hkl\}} = \frac{d_{\varphi\psi}^{\{hkl\}} - d_0^{\{hkl\}}}{d_0^{\{hkl\}}}. \quad (1)$$

where $\varepsilon_{\varphi\psi}^{\{hkl\}}$ is the measured strain for the {hkl} planes for a specimen orientation referred by the φ and ψ angles, and $d_0^{\{hkl\}}$ is the d-spacing for an unstressed specimen, usually powder. The stress tensor is considered biaxial in the irradiated layer of material (which is about 5 μm thick in the case of steel).

With the $\sin^2\psi$ method, the traditional equation for X-ray stress measurement is given as [8]:

$$\varepsilon_{\varphi\psi}^{\{hkl\}} = \frac{1}{2} S_2^{\{hkl\}} \sigma_\varphi \sin^2\psi + S_1^{\{hkl\}} (\sigma_{11} + \sigma_{22}). \quad (2)$$

where $1/2\,S_2^{\{hkl\}} = \left(1+\nu^{\{hkl\}}\right)/E^{\{hkl\}}$ and $S_1^{\{hkl\}} = -\nu^{\{hkl\}}/E^{\{hkl\}}$ are the XEC for the family of planes {hkl}, σ_{11} and σ_{22} are the stress tensor components, σ_φ is the stress in the φ direction, φ and Ψ angles are defined as the in-plane direction, and the angle between specimen normal and diffraction plane normal, respectively, as shown in Fig. 1. In Eq. 2, the strain $\varepsilon_{\varphi\psi}^{\{hkl\}}$ appears to be a linear function of $\sin^2\psi$. The differentiation of Eq. 2 with respect to $\sin^2\psi$ and the isolation of σ_φ lead to Eq. 3:

$$\sigma_\varphi = \frac{E^{\{hkl\}}}{1+\nu^{\{hkl\}}} \frac{\partial \varepsilon_{\varphi\psi}^{\{hkl\}}}{\partial \sin^2\psi} = \frac{1}{1/2\,S_2^{\{hkl\}}} \frac{\partial \varepsilon_{\varphi\psi}^{\{hkl\}}}{\partial \sin^2\psi}. \quad (3)$$

Eq. 3 shows that for the $\sin^2\psi$ method the stress σ_φ is function of the XEC, $1/2\,S_2^{\{hkl\}}$, and the linear regression between $\varepsilon_{\varphi\psi}^{\{hkl\}}$ and $\sin^2\psi$. Therefore, the $\sin^2\psi$ method implies the measurement of

Materials Research Proceedings **2** (2016) 55-60 doi: http://dx.doi.org/10.21741/9781945291173-10

strains for different ψ angles provided by the tilt of the machine. By changing ψ_0, the angle between specimen normal and incident X-ray beam, the ψ angle will subsequently change as they are fixed together by the Bragg's angle.

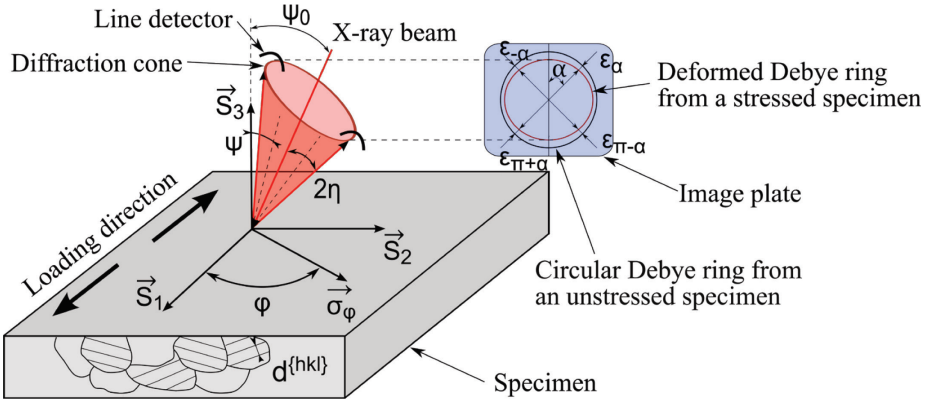

Fig. 1: Schematic representation of a specimen and grains, specimen S and measurement σ_φ *directions, diffraction cone, line detector and image plate.*

In the cos α method, the strain is determined by comparing the recorded Debye ring with the perfectly circular ring from an unstressed specimen. In fact, the strain along the normal to the diffraction planes varies with the ψ angle [1]. As the strain affects peak location, the Debye ring is not circular for specimen under stress. Eq. 4 expresses $\bar{\varepsilon}_\alpha^{\{hkl\}}$ the parameter used to calculate the stress [9]:

$$\bar{\varepsilon}_\alpha^{\{hkl\}} = \frac{1}{2}\left[\left(\varepsilon_\alpha^{\{hkl\}} - \varepsilon_{\pi+\alpha}^{\{hkl\}}\right) + \left(\varepsilon_{-\alpha}^{\{hkl\}} - \varepsilon_{\pi-\alpha}^{\{hkl\}}\right)\right]. \quad (4)$$

where $\varepsilon_\alpha^{\{hkl\}}$, $\varepsilon_{\pi+\alpha}^{\{hkl\}}$, $\varepsilon_{-\alpha}^{\{hkl\}}$, and $\varepsilon_{\pi-\alpha}^{\{hkl\}}$ are strains calculated at four points located at 90° on the Debye ring (as depicted in Fig. 1). The stress is calculated by varying α from 0° to 90° in order to cover the whole ring and is a linear function of the regression between $\bar{\varepsilon}_\alpha^{\{hkl\}}$ and cos α. As a consequence, Eq. 5 is the equation providing the stress for the cos α method:

$$\sigma_\varphi = \frac{E^{\{hkl\}}}{1+\nu^{\{hkl\}}} \frac{1}{\sin 2\eta \sin 2\psi_0} \frac{\partial \bar{\varepsilon}_\alpha^{\{hkl\}}}{\partial \cos\alpha} = \frac{1}{1/2\, S_2^{\{hkl\}}} \frac{1}{\sin 2\eta \sin 2\psi_0} \frac{\partial \bar{\varepsilon}_\alpha^{\{hkl\}}}{\partial \cos\alpha}. \quad (5)$$

where 2η is the Debye ring semi-angle.

The data are obtained for a φ angle equal to zero to estimate the uniaxial stress.

Experiment

The comparison between the two residual stress calculation methods was performed while measuring the X-ray elastic constant of a martensitic steel. The micro-tensile specimen geometry is presented in Fig. 2c). Specimen was extracted from a rolled block and contour shapes were machined with a CNC machine. Then 1 mm thick specimen was sliced using a precision cutting machine Struers Secotom-50. It was then manually polished using SiC papers (up to grade 1200) and a jig specially designed for thin specimens, allowing keeping parallelism between the two main faces. The specimen was electropolished as suggested by the ASTM standard [10]. The final specimen thickness was 0.798 mm.

Materials Research Proceedings **2** (2016) 55-60 doi: http://dx.doi.org/10.21741/9781945291173-10

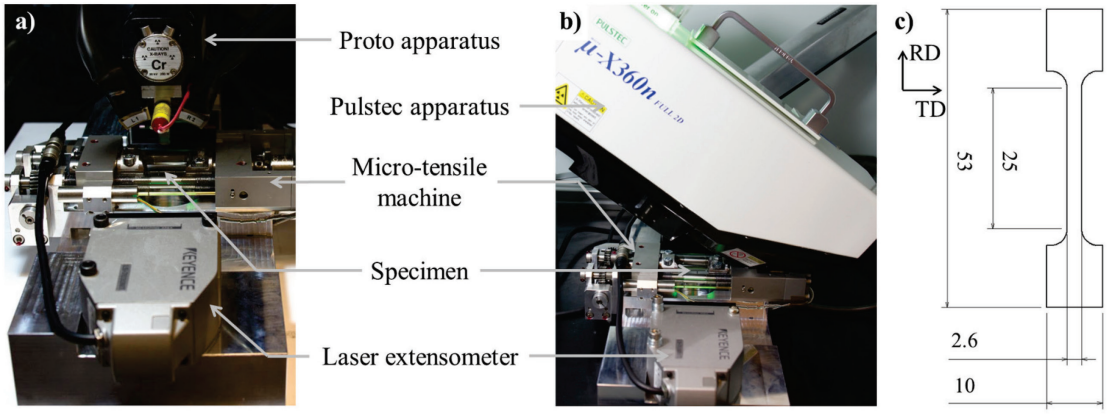

*Fig. 2: Experimental setups: micro-tensile machine and optical extensometer paired up with: a) the Proto iXRD apparatus, **b)** the Pulstec μ-X360 apparatus, and **c)** specimen geometry presentation (dimension are given in mm).*

A Proto iXRD diffractometer was used to collect the diffraction peaks for the stress calculation via the $\sin^2 \psi$ method, while the entire Debye ring was captured by a Pulstec μ-X360 apparatus for the $\cos \alpha$ method. Both machines were equipped with Cr-tube (λ = 2.291 Å). The Kα doublet from {211} planes family were used due to their high Bragg's angle (2θ = 156°), providing better accuracy on strain measurement. The Pulstec machine was set so that the ψ_0 angle is equal to 33.2° to capture the diffraction cone in a measurement of 30 s. The Proto apparatus was limited to seven different incident angles between ±13° (*i.e.* -23.6° ≤ ψ ≤ 23.6°), so the detectors do not hit the micro-tensile machine. 30 exposures of 0.25 s were used for each one of the seven incident angles, resulting in a measurement time of 53 s. All diffraction peaks were fitted using Gaussian peak fitting. In order to determine the most accurate XEC, a 0.5x3 mm^2 rectangular aperture was chosen for Proto iXRD and a 1 mm diameter aperture for Pulstec μ-X360, so the larger volume of diffracting material was used for each apparatus. The stresses were first assessed using $1/2S_{2Macro}$ = 6.50 E^{-6} MPa^{-1} calculated from the macroscopic values. The XRD measurements were repeated six times for each loading condition to test equipment repeatability.

A 5 kN micro-tensile machine, manufactured by Kammrath & Weiss GmbH, was paired up with the diffractometers in order to load the specimen in tension. Nine loading conditions were chosen from 0% to 70% of the yield strength, which has been previously determined by three macroscopic tensile tests.

Micro-tensile tests were conducted under displacement control (displacement rate of 3 $\mu m.s^{-1}$) and the displacement was stopped for the various loading dwells. The specimen elongation/contraction was continuously recorded by a Keyence LS-7030M optical extensometer during the whole experiment to assess the macroscopic strain. The experimental setup with the micro-tensile machine and the laser extensometer is presented in Fig. 2a) & b) when combined with the two XRD apparatus.

Discussion and Results

Fig. 3 presents the nominal stress-strain evolution applied during the experiment using Pulstec diffractometer. The plateaus correspond to the XRD measurement periods, *i.e.* the six measurement repetitions. The nominal stress and strain were found to be constant during these measurement periods. The difference in applied stress between the beginning of 1st measurement and the end of the 6th is less than 1MPa in average, except for the highest loading condition where the load decrease by 4.3MPa. This larger difference is due to a slightly sliding of the specimen in the grip for this specific condition. Nevertheless, the difference in load does not appear to be the main parameter affecting the stress measurement in this case as the lowest stress value was not measured for the 6th repetition.

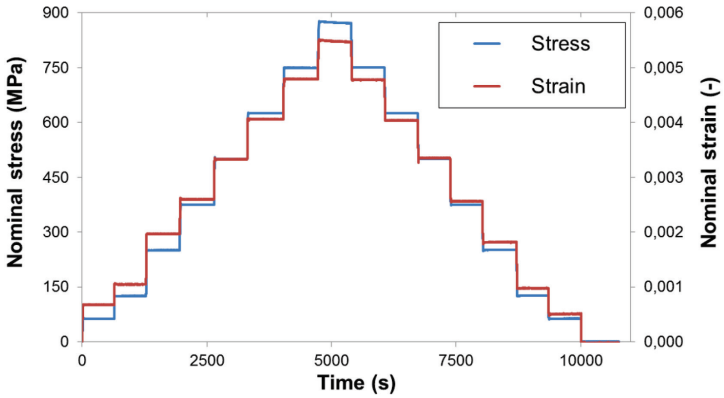

Fig. 3: Nominal stress and nominal strain evolution during the measurements with Pulstec apparatus.

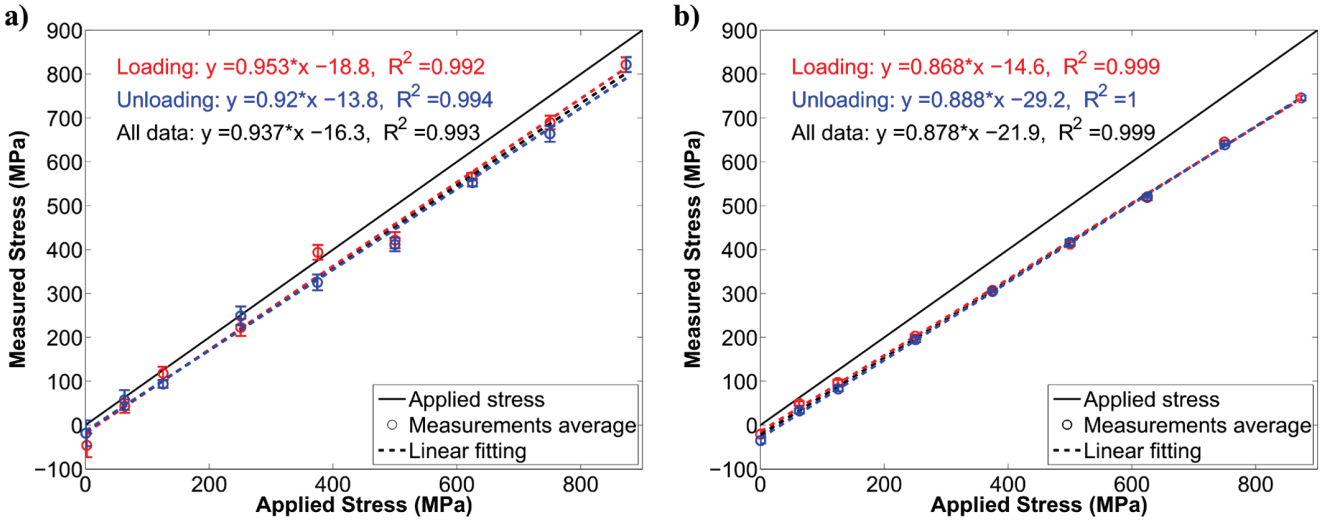

*Fig. 4: Presentation of measured stresses calculated with a) the $\sin^2\psi$ method (via Proto iXRD) and **b)** the cos α method (via Pulstec μ-X360), for the different loading conditions.*

Average stresses are plotted versus applied load, and are presented in Fig. 4 for the two stress calculation methods, therefore for the two diffractometers. The error bars correspond to a 95% confidence interval calculated using the Student's law. For both graphs, the stresses measured during loading and unloading are depicted as red and blue plots, respectively. The straight solid line represents a reference line in the hypothetical case where the XEC values can be estimated with the macroscopic mechanical constants of the material. As depicted in Fig. 4a) & b), the various plots are not aligned with this reference line showing that $1/2\,S_2^{\{211\}}$ is different from the macroscopic XEC and has to be calculated to make the data slope fit with the reference line, as proposed by Munsi et al. [11]. The correction coefficients were found to be 1.067 for the measurements done with $\sin^2\psi$ method and 1.139 for the measurements done with the cos α method. This lead to two XEC for the {211} family of planes: $1/2\,S_2^{\{211\}}{}_{\sin^2\psi} = 6.93 \pm 0.32$ MPa^{-1} and $1/2\,S_2^{\{211\}}{}_{\cos\alpha} = 7.40 \pm 0.1$ MPa^{-1}. Errors are calculated using a 95% confidence interval for the linear regression coefficients.

As exposed earlier in the Stress Analysis section, the XEC should be the same for both stress calculation methods. Consequently, the XEC previously determined should not differ from one measurement method to the next. Fig. 4 shows that the discrepancy of the results is lower with the cos α method, demonstrating a higher repeatability of this measurement. This may be due to the fact that in the current study the 2D detector captures 35 times more diffraction peaks, in a single

exposure, than the two line detectors. This provides more statistical data for the stress calculation. For $\sin^2 \psi$ method (Fig. 4a)), the large difference in fitting curves for the loading and unloading conditions may show a low accuracy. This may be explained by a too small ψ angle scan for the $\sin^2 \psi$ method, even if the volume irradiated was twice bigger for the Proto diffractometer.

Conclusions

The stresses measured by X-ray diffraction are in linear relation with the X-ray elastic constant. Therefore, a wrong XEC value may introduce a large bias in the measured stress. The use of a micro-tensile machine to stress the specimen at given macroscopic loads permits to compare the $\sin^2 \psi$ and the $\cos \alpha$ methods for stress calculation, while accessing the XEC of the studied material. Depending on the methods used for the stress calculation, a large difference in material intrinsic constant can be found. In the present study, the $\cos \alpha$ method via the 2D detector has shown a better measurement repeatability than the $\sin^2 \psi$ method via the line detectors.

Acknowledgements

The authors would like to thank the research funding from the CRIAQ project MANU508 supported by the Natural Sciences and Engineering Research Council of Canada (NSERC).

References

[1] B.D. Cullity, Elements of X-ray diffraction, Addison-Wesley Publishing Company, Inc., 1956.
[2] I.C. Noyan, J.B. Cohen, Residual stress measurement by diffraction and interpretation, Springer-Verlag, New York, 1987.
[3] S. Taira, K. Tanaka, T. Yamasaki, A method of X-ray microbeam measurement of local stress and its application to fatigue crack growth problems, Journal of the Society of Materials Science, Japan, 27 (1978), pp. 251-256 (in Japanese).
http://dx.doi.org/10.2472/jsms.27.251
[4] K. Hiratsuka, T. Sasaki, K. Seki, Y. Hirose, Development of measuring system for stress by means of image plate for laboratory X-ray experiment, JCPDS - International Centre for Diffraction Data, 46 (2003), pp. 61-67.
[5] P.S. Prevey, A method of determining the elastic properties of alloys in selected crystallographic directions for X-ray diffraction residual stress measurement, Adv. in X-ray Analysis, 20 (1977), pp. 345-354.
http://dx.doi.org/10.1007/978-1-4613-9981-0_30
[6] V. Savaria, F. Bridier, P. Bocher, Measuring in-depth residual stress gradients: the challeng of induction hardened parts, in: S.J.B. Kurz, E.J. Mittemeijer, B. Scholtes (Eds.), International Conference on Residual Stresses 9 (ICRS 9), 2014, Garmisch-Partenkirchen, Germany.
[7] V. Savaria, F. Bridier, P. Bocher, Predicting the effects of material properties gradient and residual stresses on the bending fatigue strength of induction hardened aeronautical gears, International Journal of Fatigue, 85 (2016), pp. 70-84.
http://dx.doi.org/10.1016/j.ijfatigue.2015.12.004
[8] P.S. Prevéy, X-ray diffraction residual stress technique, in: R.E. Whan (Ed.) Materials Characterization, ASM International, 1986, pp. 380-392.
[9] K. Tanaka, Y. Akiniwa, Diffraction Measurements of Residual Macrostress and Microstress Using X-Rays, Synchrotron and Neutrons, JSME International Journal Series A, 47 (2004), pp. 252-263.
http://dx.doi.org/10.1299/jsmea.47.252
[10] ASTM, E1426-98 Standard Test Method for Determining the Effective Elastic Parameter for X-Ray Diffraction Measurements of Residual Stress, 2009.
[11] A.S.M.Y. Munsi, A.J. Waddell, C.A. Walker, A Method for Determining X-ray Elastic Constants for the Measurement of Residual Stress, Strain, 39 (2003), pp. 3-10.
http://dx.doi.org/10.1046/j.1475-1305.2003.00044.x